Astron. Astrophys. 353, 813–822 (2000)

ASTRONOMY AND ASTROPHYSICS

Structure and magnetic configurations of accretion disk-dynamo models

M.v. Rekowski, G. Rüdiger, and D. Elstner

Astrophysikalisches Institut Potsdam, An der Sternwarte 16, 14482 Potsdam, Germany

Received 4 June 1999 / Accepted 8 October 1999

Abstract. The influence of large-scale magnetic fields on the structure of accretion disks is studied. The magnetic field is obtained by a self-consistent nonlinear dynamo model with magnetic pressure strongly influencing the density stratification which itself feeds back to the field generation. The resulting magnetic field geometry is discussed in relation to the accretion disk wind theory.

Regarding new results of MHD turbulence simulations, both possible signs of the α-effect are allowed (Brandenburg & Donner 1997). In the canonical case of *positive* α the resulting field is of quadrupolar symmetry. The field strength is about 50% of the value for dynamo models nonlinearly limited by α-quenching. The temperature profiles as well as the disk geometry remain nearly unchanged. The viscous stress remains the key transporter of angular momentum driving the accretion inflow.

For *negative* α, however, a stationary dipolar structure of the magnetic field results. The additional magnetic torque at the disk surface changes the profile of the effective temperature significantly to a profile which is more flat. The magnetic torque becomes of the same order as the radial viscous torque. The inclination angle of the poloidal field exceeds 30° even for a magnetic Prandtl number of order unity, and also the criterion for poloidal collimation after Spruit et al. (1997) is fulfilled. The dynamo-generated magnetic field configuration thus supports the magnetic wind launching concept for accretion disks for realistic turbulent magnetic Prandtl numbers.

Key words: accretion, accretion disks – magnetic fields – ISM: jets and outflows – turbulence

1. Motivation

The mean-field dynamo theory describes the maintenance of large-scale magnetic fields by flow patterns in conducting fluids. As is well known, in particular the feedback of the induced magnetic fields onto the fluid limits the magnetic field amplitude. While for stars the magnetic feedback basically drives internal large-scale flows ('Malkus-Proctor effect') and/or suppresses and deforms the turbulent convection ('α-quenching', '$\eta_{\rm T}$-quenching'), in galaxies and accretion disks the geometry of the disks is affected as well (Dobler et al. 1996; Rüdiger & Schultz 1997; Campbell 1997). Campbell (1999) presents disk-dynamo models with moving upper and lower boundaries as the only nonlinear feedback possibility. For given α and $\eta_{\rm T}$-effects the disk thickness is the only adjustable eigenvalue of such dynamo models which – for the given parameters – exceeds the nonmagnetic standard accretion disk thickness. The difference should be produced by the magnetic pressure, which to this end needs such high values that the magnetic transfer of angular momentum also reaches remarkable efficiency with important consequences. This is all done using an averaged vertical structure, assuming a Gaussian like profile of density.

Here we shall develop a much more complete dynamo model for accretion disks. The resulting magnetic field will both alter the turbulence and the disk structure so that the number of nonlinearities increases. Indeed, the structure of the accretion disks reflects considerable magnetic influences even if the main feedback happens via the turbulence – but the turbulence remains the key transporter of the angular momentum.

The eigenmode for an accretion disk dynamo with vacuum surrounding has quadrupole-parity for both positive and negative dynamo numbers critical for the field excitation (Torkelsson & Brandenburg 1994a; Rüdiger et al. 1994). The time regimes with slightly modified surroundings, however, strongly depend on the sign of the α-effect, if the α is positive in the northern hemisphere then the magnetic field pattern is steady and it is oscillatory for α-profiles with negative values in the north and positive in the south. For the latter case, Torkelsson & Brandenburg (1994b) even present chaotic solutions with almost dipolar parity, which, however, are not allowed to influence the accretion disk structure. We have to check our new model with magnetic-influenced density-stratification, ohmic heating and magnetic torques for its temporal character in both cases, for positive α as well as for negative α.

For strong fields the Lorentz force in the radial momentum equation could even affect the Kepler rotation law. Consequently, difficulties appear to launch winds and jets in the accretion disk halo via the Blandford & Payne (1982) mechanism as the centrifugal force driving the outflow is reduced for sub-Keplerian motion (Ogilvie & Livio 1998). Here we shall demonstrate that the geometry of the field-lines will also play

Send offprint requests to: G. Rüdiger

an important role. In particular for the launching problem dipolar solutions will strongly differ from quadrupolar solutions so that the sign of the α-effect may be responsible for the magnetic jet launching concept.

Our model further develops the standard-accretion disk dynamo model of Rüdiger et al. (1995). While again the induction equation is solved in a 2D geometry, the hydrodynamics is here formulated for a 1+1D model – embedded in the 2D domain for the induction equation – allowing for the inclusion of the magnetic pressure and Ohmic heating into the computation of the vertical structure and magnetic torques in the disk diffusion equation. Concerning the question of launching winds the model is not completely self-consistent; on the one hand we get a steady state solution for the disk diffusion equation with constant accretion rate per unit area, on the other hand the halo is assumed to rotate as the disk with Keplerian velocity, slightly contrary to the idea of magnetically accelerated material flowing along the field line corotating with its footpoint. The results, however, are spectacular with respect to the inclination angle of the magnetic fieldlines with the rotation axis. While any magnetic dragging of an external field by the accretion flow only provides suitable inclination angles for very high magnetic Prandtl number ($\mathrm{Pm} \gg 1$), the presented dynamo solution with dipolar symmetry already yields the same angles for Pm=1. The particular dynamo model (with negative α-effect) can thus be understood as a model for the acceleration of magnetic winds or jets.

2. The turbulent EMF

The evolution of the mean magnetic field $\bar{\boldsymbol{B}}$ is governed by the dynamo equation

$$\frac{\partial \bar{\boldsymbol{B}}}{\partial t} = \mathrm{rot}\ (\bar{\boldsymbol{u}} \times \bar{\boldsymbol{B}} + \boldsymbol{\mathcal{E}}), \tag{1}$$

where $\boldsymbol{\mathcal{E}}$ is the turbulent electromotive force, $\boldsymbol{\mathcal{E}} = \langle \boldsymbol{u}' \times \boldsymbol{B}' \rangle$, and $\bar{\boldsymbol{u}}$ the mean velocity. We employ cylindrical polar coordinates (R, ϕ, Z) and assume axisymmetry, $\partial/\partial\phi = 0$. The magnetic diffusivity is negligible in comparison with the turbulent diffusion.

We assume approximate scale separation and write

$$\mathcal{E}_i = \alpha_{ij} \bar{B}_j + \eta_{ijk} \bar{B}_{j,k} + ... \tag{2}$$

The α-tensor is anisotropic, even in the case of slow rotation where the correlation time τ_{corr} is short compared with the rotation period τ_{rot}. $\boldsymbol{\Omega}$ is the basic rotation measured in terms of the Coriolis number $\Omega^* = 2\ \tau_{\mathrm{corr}} \Omega$.

The turbulent magnetic diffusivity tensor exists even without basic rotation. In the absence of any anisotropies it is simply $\eta_{ijk} = \eta_{\mathrm{T}} \epsilon_{ijk}$. For slow rotation and weak magnetic field the eddy diffusivity tensor takes the simple form $\eta_{ijk} = \eta_{\mathrm{T}} \epsilon_{ijk}$ so that

$$\boldsymbol{\mathcal{E}} = -\eta_{\mathrm{T}}\, \mathrm{rot}\, \bar{\boldsymbol{B}}. \tag{3}$$

The reference value for the eddy diffusivity is

$$\eta_0 = \nu_0/\mathrm{Pm}. \tag{4}$$

We shall work here with the traditional value of Pm = 1 and without the effect of the 'η-quenching'.

2.1. The α-tensor

The α-effect is mainly due to the rotational influence on the turbulence in stratified media. Density stratification as well as turbulence intensity can provide the required inhomogeneity. We shall work here only *with pure density stratification* and assume an approximation in which only terms linear in the density gradient are included.

Kitchatinov (1991) derived the advection-type parts of the α-tensor. Rüdiger & Kitchatinov (1993) did the same with the symmetric part of the tensor. The α-effect itself is odd in the angular velocity. The chosen turbulence model was identical in both papers and it closely resembles the mixing-length theory. It describes a "quasi-isotropic" turbulence, which is isotropic over small distances and anisotropic over large ones. The latter effect is due to the density stratification.

Then the α-tensor has the structure

$$\alpha_{ij} = -\alpha_{ij} \frac{\partial \log \rho}{\partial Z} \langle \boldsymbol{u}'^2 \rangle \tau_{\mathrm{corr}}, \tag{5}$$

with

$$\alpha = c_\alpha \begin{pmatrix} \frac{2}{5}\psi & 0 & 0 \\ 0 & \frac{2}{5}\psi & 0 \\ 0 & 0 & -\frac{2}{15}\psi_Z \end{pmatrix} \Omega^*. \tag{6}$$

Currently there is no information about the true vertical stratification of the turbulence intensity in accretion disks. Therefore, the contribution of the vertical distribution of the turbulence intensity to the α-effect is neglected in (5) and so our results only hold for a turbulent velocity field satisfying $\partial \langle \boldsymbol{u}'^2 \rangle / \partial Z = 0$.

From the expressions given by Rüdiger & Kitchatinov (1993),

$$\psi = \frac{5}{4\Omega^{*4}} \left(\Omega^{*2} + 6 - \frac{6 + 3\Omega^{*2} - \Omega^{*4}}{\Omega^*}\ \arctan \Omega^* \right) \tag{7}$$

and

$$\psi_Z = -\frac{15}{4\Omega^{*4}} \left(-\frac{10\Omega^{*2} + 12}{1 + \Omega^{*2}} + \frac{2\Omega^{*2} + 12}{\Omega^*}\ \arctan \Omega^* \right) \tag{8}$$

in full Coriolis number dependence can be derived.

The given terms represent the traditional α-effect; they are all odd in Ω. Note that for large Ω^*, the function ψ runs with $1/\Omega^*$.

As usual in the accretion disk turbulence the eddy viscosity $\nu_{\mathrm{T}} = c_\nu \langle \boldsymbol{u}'^2 \rangle\ \tau_{\mathrm{corr}}$ is parameterized via

$$\nu_{\mathrm{T}} = \alpha_{\mathrm{SS}} H^2 \Omega \tag{9}$$

in the non-magnetized case with H as the half-thickness of the accretion disk (Shakura & Sunyaev 1973; Pringle 1981). Obviously,

$$\langle \boldsymbol{u}'^2 \rangle\ \tau_{\mathrm{corr}} = \frac{\alpha_{\mathrm{SS}}}{c_\nu}\ H^2 \Omega, \tag{10}$$

hence

$$\alpha_{RR} = \alpha_{\phi\phi} = \frac{2 c_\alpha \alpha_{\mathrm{SS}} \Omega^* \psi}{5 c_\nu}\ z\Omega,$$

$$\alpha_{ZZ} = -\frac{c_\alpha 2 \alpha_{\mathrm{SS}} \Omega^* \psi_z}{15 c_\nu}\ z\Omega. \tag{11}$$

With quite the same philosophy the eddy diffusivity in the accretion disk must be written as

$$\eta_{\rm T} = \frac{\alpha_{\rm SS}\Phi}{\rm Pm} H^2 \Omega \tag{12}$$

with

$$\Phi = \frac{3}{4\Omega^{*2}} \left(1 + \frac{\Omega^{*2}-1}{\Omega^*} \arctan \Omega^*\right) \tag{13}$$

(Kitchatinov et al. 1994).

2.2. Magnetic feedback onto the turbulence

In the case of a thin disk geometry, the customary definition of the dynamo number $\mathcal{D}$ is

$$\mathcal{D} = \frac{\alpha_{\phi\phi}(z=H)\,\Omega\,H^3}{\eta_{\rm T}^2}. \tag{14}$$

With our parameterization of the properties of the turbulence, $\mathcal{D}$ does not depend on radius (Stepinski & Levy 1990). The dynamo number is completely determined by $\alpha_{\rm SS}$ and the magnetic Prandtl number Pm,

$$\mathcal{D} \propto \frac{{\rm Pm}^2}{\alpha_{\rm SS}}, \tag{15}$$

and does not change in our model when the magnetic field feeds back to the disk structure because of the definition of turbulent magnetic diffusivity (12). We consider only the back-reaction of the generated magnetic field on the α-effect, ignoring any possible back-reaction of the magnetic field on the magnetic diffusivity. The nonlinearity is introduced in the form of

$$\alpha = \frac{\alpha_0}{1+\beta^2}, \tag{16}$$

with the property of reducing the helicity of turbulence with increasing magnitude of the magnetic field. β is the large-scale magnetic field normalized with its equipartition value, $\beta = |\bar{\boldsymbol{B}}|/B_{\rm eq}$ with $B_{\rm eq} = \sqrt{\mu_0 \rho \langle \boldsymbol{u}'^2\rangle}/c_{\rm eq}$. The damping parameter is of order unity, we have worked here with $c_{\rm eq} = 3$.

3. Basic equations

3.1. Hydrodynamics

In Livio & Pringle (1992) a toroidal field is induced by the *vertical* gradient of the angular velocity computed in the system corotating with the star. In our calculations the predominantly toroidal component of the magnetic field is induced by differential rotation of the poloidal field governed by a dynamo process. The magnetic pressure formed by the toroidal field acts in vertical as well as radial direction with consequences for the thickness and the rotation law of the disk. Additionally, there is an angular momentum transport by the Maxwell stress which may easily act as a driver of the overall inward accretion flow. These terms are derived below.

In cylinder coordinates the conservation law of mass reads

$$\frac{\partial \rho}{\partial t} + \frac{1}{R}\frac{\partial}{\partial R}(R\rho\bar{u}_R) + \frac{\partial}{\partial Z}(\rho\bar{u}_Z) = 0. \tag{17}$$

Integration over Z yields

$$\frac{\partial \Sigma}{\partial t} + \frac{1}{R}\frac{\partial}{\partial R}\big(R\Sigma\bar{u}_R\big) = 0, \tag{18}$$

or in the stationary case $2\pi R\Sigma\bar{u}_R = -\dot{M}$ with

$$\Sigma = \int\limits_{-\infty}^{\infty} \rho dZ. \tag{19}$$

The magnetic field appears in the momentum equation. Its radial part provides

$$\rho\,\frac{\partial \bar{u}_R}{\partial t} + \rho\bar{u}_R\frac{\partial \bar{u}_R}{\partial R} + \frac{\partial p}{\partial R} + \frac{1}{3}\frac{\partial}{\partial R}\big(\rho\langle \boldsymbol{u}'^2\rangle\big) - \rho R\Omega^2 = \\ = -GM\frac{\rho}{R^2} - \frac{1}{2\mu_0}\frac{\partial}{\partial R}\left(B_\phi^2 + B_Z^2 - B_R^2\right). \tag{20}$$

Here M is the central mass and p the gas pressure. If all terms could be neglected except centrifugal force and central gravitation, the Kepler law $\Omega_{\rm K} = \sqrt{GM/R^3}$ results. Assuming that the central radial gravitation in the disk is only balanced by the centrifugal force and magnetic pressure force, integration of (20) over Z yields

$$\left(-\frac{GM}{R^2} + R\Omega^2\right)\Sigma + \mathcal{B}_R = 0 \tag{21}$$

with

$$\mathcal{B}_R = \frac{1}{2\mu_0}\frac{\partial}{\partial R}\int\limits_{-\infty}^{\infty}\left(B_R^2 - B_\phi^2 - B_Z^2\right) dZ. \tag{22}$$

From (21) the angular velocity reads $\Omega = \sqrt{\Omega_{\rm K}^2 - \mathcal{B}_R/R\Sigma}$. The conservation law of angular momentum is the ϕ-component of the Reynolds equation, i.e.

$$\frac{\partial}{\partial t}(\rho R^2\Omega) + {\rm div}\,\boldsymbol{t} = 0 \tag{23}$$

with

$$\boldsymbol{t} = \rho R^2\Omega\bar{\boldsymbol{u}} + \rho R\langle u'_\phi \boldsymbol{u}'\rangle - \frac{R}{\mu_0}B_\phi\boldsymbol{B}. \tag{24}$$

As usual the basic stress-strain relation

$$\langle u'_i u'_j\rangle = \frac{1}{3}\langle \boldsymbol{u}'^2\rangle\delta_{ij} - \nu_{\rm T}(\bar{u}_{i,j} + \bar{u}_{j,i}) \tag{25}$$

is used, so that after Z-integration

$$\frac{\partial}{\partial t}(\Sigma R^2\Omega) + \frac{1}{R}\frac{\partial}{\partial R}\left(\Sigma R^3\left(\Omega\bar{u}_R - \nu_{\rm T}\frac{\partial\Omega}{\partial R}\right)\right) = \mathcal{B}_\phi \tag{26}$$

results. The magnetic torque $\mathcal{B}_\phi$ is

$$\mathcal{B}_\phi = \frac{2R}{\mu_0}\,B_Z\,B_\phi^{\rm surf} + \frac{1}{\mu_0 R}\frac{\partial}{\partial R}\left(R^2\int\limits_{-\infty}^{\infty} B_R B_\phi dZ\right), \tag{27}$$

where the magnetic field in the first term of the RHS must be taken at the disk surface. Elimination of the radial inflow velocity from Eqs. (18) and (26) gives a generalization of the disk diffusion relation, i.e.

$$\frac{\partial \Sigma}{\partial t} + \frac{1}{R}\frac{\partial}{\partial R}\left\{ \frac{\mathcal{B}_\phi + \frac{1}{R}\frac{\partial}{\partial R}(\nu_\mathrm{T}\Sigma R^3 \frac{\partial \Omega}{\partial R})}{\frac{1}{R}\frac{\partial}{\partial R}(R^2\Omega)} \right\} = 0. \tag{28}$$

The magnetic field, however, does not only form large-scale Lorentz forces but it also influences the eddy viscosity in Eq. (28).

3.2. Thermodynamics

The general heat transport equation is

$$\rho T \frac{dS}{dt} = \rho\varepsilon - \mathrm{div}\, \boldsymbol{F}, \tag{29}$$

with $\boldsymbol{F}$ as the total heat flux vector and ε as the frictional heat production rate

$$\varepsilon = \nu\big(u_{i,k} + u_{k,i}\big)^2. \tag{30}$$

In the stationary case under the inclusion of turbulence, Eq. (30) becomes

$$\rho\nu_\mathrm{T}\big(\bar{u}_{i,k} + \bar{u}_{k,i}\big)^2 + \mu_0\eta_\mathrm{T}\boldsymbol{J}^2 = \mathrm{div}\, \boldsymbol{F} \tag{31}$$

or, after an integration over Z,

$$\nu_\mathrm{T}\Sigma\left(R\frac{\partial\Omega}{\partial R}\right)^2 + \mu_0\eta_\mathrm{T}\int\limits_{-\infty}^{\infty}\boldsymbol{J}^2 dZ = 2Q^- \tag{32}$$

with

$$Q^- = \sigma T_\mathrm{eff}^4 \tag{33}$$

and the electrical current $\boldsymbol{J} = \mathrm{rot}\,\bar{\boldsymbol{B}}/\mu_0$.
It remains to compute the vertical structure of the disk. To this end the standard procedure can be used. For thin disks the energy equation (31) becomes

$$\frac{\partial F}{\partial Z} = \nu_\mathrm{T}\rho\left(R\frac{\partial\Omega}{\partial R}\right)^2 + \mu_0\eta_\mathrm{T}\boldsymbol{J}^2, \tag{34}$$

where the vertical component F of the heat-flux vector after the diffusion approximation is

$$F = -\frac{16\sigma T^3}{3\kappa\rho}\frac{\partial T}{\partial Z}. \tag{35}$$

The vertical stratification in its simplest formulation but with inclusion of the magnetic pressure is

$$\frac{\partial}{\partial Z}\left(p + \frac{B_\phi^2}{2\mu_0}\right) = -\rho\Omega_\mathrm{K}^2 Z, \tag{36}$$

by which also the disk height H will be defined. The corresponding boundary conditions are $F(Z=0) = 0$ and

$$F(H) = Q^-, \qquad T(H) = \frac{\sqrt[4]{Q^-}}{\sigma}, \qquad \tau(H) = 2/3. \tag{37}$$

The latter relation can be reformulated as

$$p\big|_\mathrm{surf}\,\kappa_\mathrm{surf} = \frac{2}{3}\,\Omega_\mathrm{K}^2(R)H. \tag{38}$$

For the opacity we use Kramers' law $\kappa = 6.6 \cdot 10^{22}\ \rho T^{-3.5}$ c.g.s. (Meyer & Meyer-Hofmeister 1982; Smak 1984).

3.3. The inflow

By comparison with the mass conservation law (18) the accretion flow $\bar{u}_R$ can be read from (28) as

$$\bar{u}_R = \bar{u}_R^\mathrm{visc} + \bar{u}_R^\mathrm{mag} \tag{39}$$

with the viscous velocity

$$\bar{u}_R^\mathrm{visc} = \frac{1}{R\Sigma}\frac{\frac{1}{R}\frac{\partial}{\partial R}(\nu_\mathrm{T}\Sigma R^3\frac{\partial\Omega}{\partial R})}{\frac{1}{R}\frac{\partial}{\partial R}(R^2\Omega)} \tag{40}$$

and the magnetically driven velocity

$$\bar{u}_R^\mathrm{mag} = \frac{1}{R\Sigma}\frac{\mathcal{B}_\phi}{\frac{1}{R}\frac{\partial}{\partial R}(R^2\Omega)}. \tag{41}$$

For Kepler rotation,

$$\bar{u}_R = \frac{1}{R\Sigma}\left(\frac{2\mathcal{B}_\phi}{\Omega} - \frac{4}{3}\sqrt{R}\frac{\partial}{\partial R}\left(\frac{\sqrt{R}}{\Omega^2}\left(2Q^- - \mu_0\eta_\mathrm{T}\int\limits_{-\infty}^{\infty}\boldsymbol{J}^2 dZ\right)\right)\right), \tag{42}$$

which must be used in the induction equation (1). Various vertical profiles for the radial flow have been applied, among them also the profile derived by Kley & Lin (1992).
In general, a vertical profile of $\bar{u}_R$ leads to the dragging mechanism of vertical magnetic field in the disk which will be transformed to the toroidal field by differential rotation. The generation of B_R from B_Z via a vertical shear of u_R can be described by the magnetic Prandtl number

$$\frac{|B_R|}{|B_Z|} \approx -\frac{\bar{u}_R H}{\eta_\mathrm{T}} \approx \frac{\nu_\mathrm{T}}{\eta_\mathrm{T}}\frac{H}{R} = \mathrm{Pm}\frac{H}{R}, \tag{43}$$

where the factor of proportionality is about 1.5. It is obvious that for low magnetic Prandtl numbers $\mathrm{Pm} \leq 1$ and thin disks with the usual ratio H/R of a few percent the dragging mechanism and therefore the vertical profile of the inflow velocity has no significant influence of the field evolution. This was also a result of Reyes-Ruiz & Stepinski (1996) who used a vertical averaged $\bar{u}_R$ within the disk, falling to zero in the halo. Significant bending is only reached for magnetic Prandtl numbers in the order of 10^2. The vertical component of the velocity field in our model is ignored because it is small in thin disks.

3.4. Boundary conditions

We have to specify two boundary conditions for the disk diffusion equation which is of second order in Σ. According to the

steady state standard disk solution we set the constant accretion rate $\dot{M}$ at the outer edge of the disk and the no-torque condition at the inner edge of the disk which is localized at the stellar surface (Kley 1989; Duschl & Tscharnuter 1991; Regev & Bertout 1995; v. Rekowski & Fröhlich 1997; Wang 1995, 1997; Brandenburg & Campbell 1998). The disk is embedded in a two dimensional non-equidistant grid for the induction equation, where the halo – the regime outside the optical thick disk – is assumed to be a vacuum. This is modelled by a very large fraction of the turbulent magnetic diffusivity $\eta_{\rm out}$ in comparison to its value $\eta_{\rm disk}$ inside the disk: $\epsilon = \eta_{\rm out}/\eta_{\rm disk} = 100$. In the real vacuum case the surface term in the magnetic torque of Eq. (27) disappears because B_ϕ has to be zero in case of axisymmetric solutions.

Integration of the stationary disk diffusion equation leads to the first integration constant $\dot{M}$ and to the second constant C which represents the specific total flux of angular momentum

$$C = \frac{2\pi}{\dot{M}}\nu_{\rm T}\Sigma R^3\frac{\partial\Omega}{\partial R} + \frac{2\pi}{\dot{M}}\frac{1}{\mu_0}R^2\int\limits_{-\infty}^{\infty} B_R B_\phi dZ + R^2\Omega, \quad (44)$$

which can be normalized further to the reference value for Keplerian rotation at the stellar surface $\mathcal{C} \equiv C/(\Omega_{\rm K*}R_*^2)$.

The no-torque condition $\mathcal{C} = 1$ is equivalent to assuming that there is a net flux of angular momentum, $\dot{I} = \dot{M}(GMR_*)^{\frac{1}{2}}$, from the disk to the star which is the maximal value. This leads to the fact that both the radial viscous and magnetic angular momentum transport have to be zero separately at the disk inner edge because they have the same direction. As is shown in a detailed study of the full boundary problem (M. v. Rekowski & Fröhlich 1997) the disk surface density nearly vanishes in the region between star and disk which leads automatically to a flux of angular momentum $\mathcal{C} \approx 1.03$ which is not far from the flux concerning the no-torque condition of the standard disk solution. The condition for the magnetic angular momentum transport is fulfilled by prescribing the infinite-conductor ($B_{\rm tang}$ = 0, $E_{\rm vert}$ = 0), where here B_R vanishes as well as the pseudo-vacuum condition ($B_{\rm vert}$ = 0, $E_{\rm tang} = 0$), where B_ϕ vanishes. In our model calculations we set the condition for perfect conductor at the inner edge – the region between star and disk – and the pseudo-vacuum condition at the radial outer boundaries and the vertical boundaries.

4. Results

The numerical computations have been performed assuming a White Dwarf of 1 solar mass, with a radius of 10^9 cm, and an accretion rate of $\dot{M} = 10^{-10}\,M_\odot$/yr (Horne 1993). The turbulence parameters are $\alpha_{\rm SS} = 0.01$, $\Omega^* = 10$. The magnetic Prandtl number $\rm Pm$ is taken as unity. The disk with the aspect ratio H/R less than 0.02 is embedded in a 2D non-equidistant grid for the induction equation which takes 10 stellar radii in radial and 15 stellar radii in vertical direction. By using such a high vertical ratio – compared to the disk height – it is satisfied that the vertical outer boundary condition does not play a significant role on the field evolution inside.

We used 46×74 gridpoints in the R, Z plane where in Z direction at least 30 gridpoints are settled within the whole disk. These values were doubled for test calculations. Also a comparison with an equidistant grid on a part of our computational domain was performed. The ratio between maximal and minimal grid width in R direction is about 10 and in Z direction 500. In the inner regions of the disk the vertical gridsize changes only in the halo. The non-equidistant physical grid is analytically transformed to an equidistant grid. The transformed induction equation is then solved on the equidistant grid. So we don't loose any accuracy of the difference formulas. Most of the calculations are done by solving the induction equation for the magnetic field. For the field line representation we used a slightly modified solver, which simultaneously updates the potential of the magnetic field. For the radial inner boundary condition we tested also a pseudo vacuum condition, which gave only slight differences in the very inner region of the disk to the calculations presented here.

All numerical calculations have been done for both the positive and negative dynamo-α model where the ratio of turbulent magnetic diffusivity between halo and disk is $\epsilon = 100$. For the negative dynamo number, $c_\alpha = -1$, we also have done (kinematic) calculations with $\epsilon = 10$ and $\epsilon = 1$.

As always the radial magnetic force $\mathcal{B}_R$ in Eq. (21) is still small compared with the gravitational force, it is justified to prescribe the Keplerian rotation law in the disk diffusion equation (28).

4.1. Positive dynamo number, $c_\alpha = 1$

The dynamo model for positive dynamo-α always generates a stationary magnetic field with symmetric (quadrupolar) equatorial symmetry. The field is confined to the disk, it is predominantly toroidal where its maximum value is achieved at the midplane of the disk, close to the inner edge.

In the following we will derive an estimation of the amount of the magnetic quantities against the viscous or thermal quantities for our standard disk dynamo model ($c_\alpha = +1$). In our turbulence model the dynamo number yields

$$D = \frac{2}{5}\psi(\Omega^*)\Omega^*\frac{{\rm Pm}^2}{\alpha_{\rm SS}\Phi^2(\Omega^*)c_\nu}, \quad (45)$$

where ψ is the function of Eq. (7), describing the α-effect in its dependence on the Coriolis number. Because of the chosen ansatz for the magnetic diffusivity, (12), the dynamo number is still independent of the disk geometry, it depends only on the turbulence parameters $\alpha_{\rm SS}$, Pm, Ω^* (cf. Eq. (12)).

Using the α-quenching mechanism we know that in the case of a positive α-effect ($c_\alpha = +1$) the magnetic field strength is proportional to the equipartition field, i.e.

$$|B_\phi| \propto D^{\frac{1}{2}}\,B_{\rm eq}. \quad (46)$$

On the other hand we know the production rate of toroidal field from B_R via differential rotation, i.e. $B_\phi = -C_\Omega \cdot B_R$. If the thin-disk approximation is still valid we can express the magnetic quantities as the corresponding viscous ones using

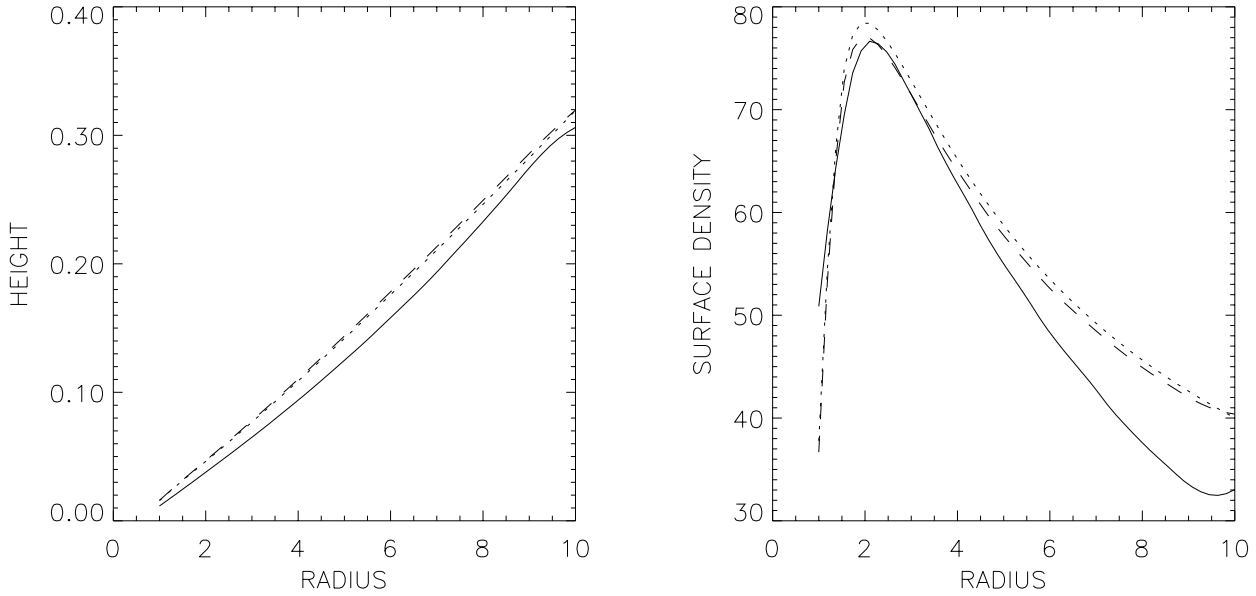

Fig. 1. Disk semi-thickness H in units of the stellar radius (LEFT) and surface density Σ in g/cm^2 (RIGHT). Pm=1, $\alpha_{\rm SS} = 0.01$, $c_\alpha = -1$ (solid), $c_\alpha = +1$ (dashed), $c_\alpha = 0$ (dotted). Height and radius are given in units of the stellar radius

the usual way to determine vertical integrals and derivatives neglecting numerical factors

$$\frac{\frac{R}{\mu_0}\int_{-H}^{H} B_R B_\phi \, dZ}{\nu_{\rm T}\Sigma R^2 \frac{\partial\Omega}{\partial R}} \propto {\rm Pm}, \qquad \frac{\frac{\partial p}{\partial Z}^{\rm mag}}{\frac{\partial p}{\partial Z}} \propto {\rm Pm}^2. \tag{47}$$

The proportionality factor is independent of the Shakura-Sunyaev parameter $\alpha_{\rm SS}$ and of the order 10^{-2} in both cases. Only an increase of ${\rm Pm}$ increases the influence of the magnetic field on the disk structure. The vertical structure will be altered because of the quadratically dependency on ${\rm Pm}$. The ratio of the radial magnetic quantities to the viscous ones depends only linearly on ${\rm Pm}$. Therefore, the influence of the magnetic field on the disk structure has an effect predominantly on the vertical structure.

The simulations confirm the estimates. For ${\rm Pm} = 1$ the magnetic quantities remain rather small compared with the viscous or thermal ones. The magnetic pressure force is less than 5% of the gas pressure except in the uppermost layers in the vertical direction. Also magnetic heating and magnetic angular momentum transfer remain negligible against their viscous counterparts (Figs. 3, 4). These ratios are in the order of 10^{-3}. The above results are indeed independent of the viscosity $\alpha_{\rm SS}$, see Table 1. The Reynolds stress remains the key transporter of angular momentum outwards which finally drives the accretion process. The influence of the Lorentz force on the disk structure in comparison to the structure of the stationary hydrodynamical solution is also small. The disk tends to extend and to become less massive (Fig. 1).

4.2. Negative dynamo number, $c_\alpha = -1$

The dynamo model with negative c_α always generates a stationary magnetic field with antisymmetric (dipolar) equatorial symmetry. The field is predominantly toroidal and its maximum value is achieved outside of the disk, depending on the ratio $\epsilon = \eta_{\rm out}/\eta_{\rm disk}$, close to the inner edge. The greater ϵ the smaller is the toroidal field in the halo. Increasing ϵ to infinity should lead to the solution for vacuum where the toroidal component in the halo vanishes. Simulating the vacuum case by setting the pseudo-vacuum condition directly at the surface of the disk we get a chaotic oscillating mode of quadrupolar type which is also already predicted by Campbell (1997). In this case, however, we are not able to calculate the structure of the magnetic field in the halo with its consequence for the jet-launching. Nevertheless, the conductivity of the halo is still unknown and certainly not zero. Note that also the geometry of the disk, concerning the ratio H/R, is important for the symmetry behaviour of the dynamo generated field. An overestimation of the disk height leads to solutions with even parity. With our non-equidistant grid, however, we are able to consider disks with realistic heights as well as high aspect ratios.

Because ϵ is finite, the toroidal component does not vanish at the disk surface but reaches its maximum in the halo and then slightly decreases to zero in vertical direction. So, the field generation cannot be understood by the same definition of the dynamo number such as in (46). The growth rate of the magnetic field happens on timescales of the diffusion time. The smaller the diffusivity in the halo the longer it takes that the magnetic field is saturated.

Contrary to the positive dynamo-number model the magnetic pressure works as an additional gravity in the hydrostatical equilibrium which has to be balanced by a stronger thermal

Table 1. The accretion disk dynamo solution for $\Omega^* = 10$, $\mathrm{Pm} = 1$, $c_\alpha = +1$. The values are taken close to the inner edge. The superscript ^{0} denotes the corresponding nonmagnetic solution

$\alpha_{\rm SS}$	$T_{\rm eff}$ [K]	H^0 [cm]	Σ^0 [g/cm^2]	B [Gauss]	β	$\frac{p^{\rm mag}}{p^{\rm gas}}$	$\frac{T_{\rm eff}}{T^0_{\rm eff}}$	$\frac{H}{H^0}$	$\frac{\Sigma}{\Sigma^0}$	$\frac{u_R}{u^0_R}$
10^{-1}	19000	$1.1 \cdot 10^7$	15.5	800	0.5	0.05	1.	1.005	0.992	1.010
10^{-2}	19000	$1.6 \cdot 10^7$	80.0	2100	1.5	0.30	1.	1.013	0.982	1.025
10^{-3}	19000	$2.1 \cdot 10^7$	440.0	5650	4.5	2.00	1.	1.030	0.942	1.062

Table 2. The same as in Table 1 but for $c_\alpha = -1$.

$\alpha_{\rm SS}$	$T_{\rm eff}$ [K]	H^0 [cm]	Σ^0 [g/cm^2]	B [Gauss]	β	$\frac{p^{\rm mag}}{p^{\rm gas}}$	$\frac{T_{\rm eff}}{T^0_{\rm eff}}$	$\frac{H}{H^0}$	$\frac{\Sigma}{\Sigma^0}$	$\frac{u_R}{u^0_R}$
10^{-1}	19000	$1.1 \cdot 10^7$	15.5	11000	8.5	$\lesssim 35.$	0.75	0.85	0.85	1.20
10^{-2}	19000	$1.6 \cdot 10^7$	80.	24000	28.0	$\lesssim 45.$	0.75	0.85	0.90	1.10
10^{-3}	19000	$2.1 \cdot 10^7$	440.	53500	45.5	$\lesssim 40.$	0.85	0.85	1.15	0.85

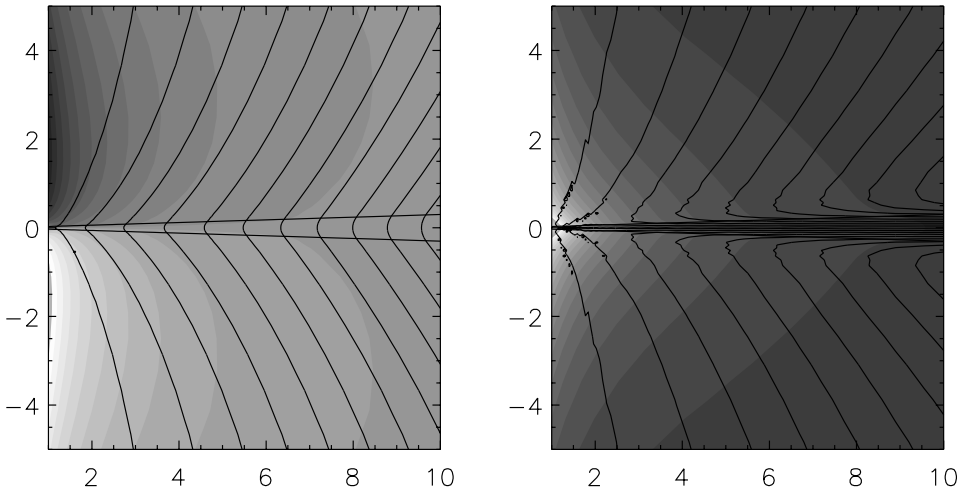

Fig. 2. The poloidal field lines for $c_\alpha = -1$ (LEFT, dipolar symmetry) and $c_\alpha = 1$ (RIGHT, quadrupolar symmetry)

pressure gradient. This can be done by a strong decrease of the disk height or a strong increase of (surface) density.

The numerical simulations show that the radial magnetic angular momentum transport is negligible in comparison to the viscous one, as in the case of positive α-effect. Also in this model the vertical gradient of the magnetic pressure first changes the vertical structure. It reaches the same order as the thermal pressure force for the chosen model parameters of turbulence (Fig. 5). The resulting disk height is about 85% of the height of a nonmagnetic disk. The behaviour of the surface density can be understood as the influence of the magnetic surface torque. The magnetic surface torque in the angular momentum equation does not vanish in this model, but is in the same order as the radial viscous torque (Fig. 6). It transports angular momentum into the halo and drives the accretion process. The effect is demonstrated in Fig. 1. The surface density is strongly decreased. Therefore, viscous torque is strongly replaced by the magnetic surface torque.

Contrary to the radial magnetic torque which can be compared with the magnetic heating term, the surface torque has no corresponding term in the energy balance, which leads to a reduction of the effective temperature because viscous shear is reduced (Fig. 8).

Our numerical calculations show that for the negative dynamo-α model the resulting magnetic field is of dipolar structure where indeed the field has a poloidal component outside of the disk which is not negligible but in the same order as within the disk. Fig. 2 shows the poloidal field structure with prescribed Keplerian velocity in the disk as well as in the halo. Due to the fact that differential rotation is also working, the toroidal field does not vanish in the halo of the disk but slightly decreases to zero in z-direction.

As shown in Figs. 6 and 7 the resulting magnetic torque is negative as required to drive inflow through the disk. The magnetic surface torque is of the same order as the radial viscous one and does not depend on the diffusivity of the surrounding halo (see Fig. 7).

5. Jet-launching

5.1. Toroidal collimation

If an accretion disk has a poloidal field and a hot corona the possibility arises to launch a magnetically-driven wind or jet. Once driven by thermal pressure gradients, mass is accelerated centrifugally along the magnetic field lines assuming that the matter along the field line is corotating with the Keplerian ve-

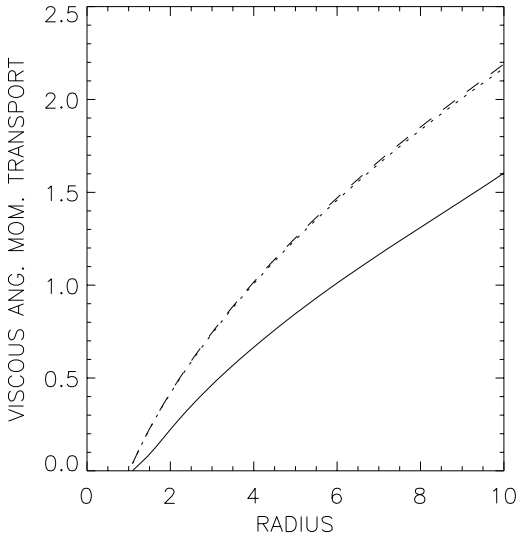

Fig. 3. The angular momentum transport by viscosity, $R\,\tilde{t}_R^{\rm visc}$, (in units of $R_*^2\Omega_{\rm K*}\dot{M}/2\pi$, the total angular momentum flux on the star at the inner edge of the disk). $c_\alpha = -1$ (solid), $c_\alpha = +1$ (dashed), $c_\alpha = 0$ (dotted)

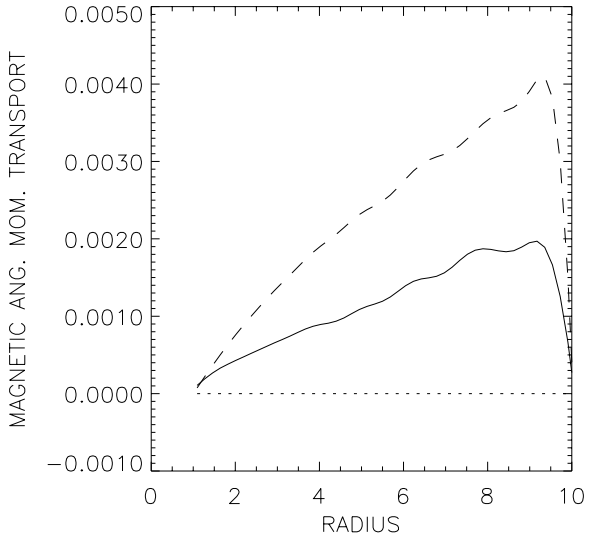

Fig. 4. The magnetic angular momentum transport (in units of $R_*^2\Omega_{\rm K*}\dot{M}/2\pi$). $c_\alpha = -1$ (solid), $c_\alpha = 1$ (dashed), $c_\alpha = 0$ (dotted). Note the small magnitude of only 1% of the viscous angular momentum transport

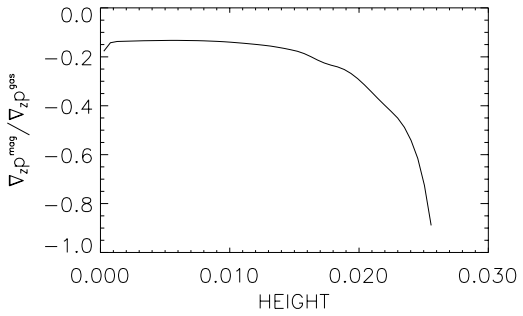

Fig. 5. Negative dynamo number ($c_\alpha = -1$): The ratio between magnetic pressure force and thermal pressure force at a radius close to the stellar surface.

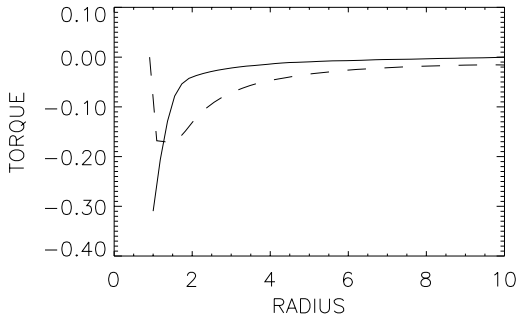

Fig. 6. Negative dynamo number ($c_\alpha = -1$): The magnetic surface torque (47) (solid) and the viscous torque (dashed), in units of $\Omega_{\rm K*}\dot{M}/2\pi$

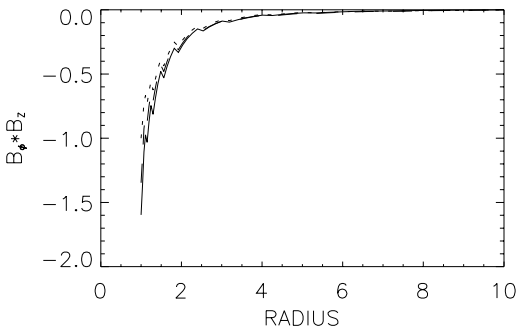

Fig. 7. Negative dynamo number ($c_\alpha = -1$): The product of toroidal field B_ϕ and vertical poloidal field B_Z at the disk surface. No influence of the halo approximation for the resulting magnetic surface torque exists: $\epsilon = 100$ (solid), $\epsilon = 10$ (dashed), $\epsilon = 1$ (dotted)

locity of the footpoint. As long as the kinetic energy density of the outflowing material is small compared to the poloidal magnetic energy density the field line will be only slightly distorted by the flow. This situation changes at the Alfvén points. If the Alfvén velocity is reached before magnetic coronal loop starts to close, the field line will be dragged outwards with the flow (Campbell 1997). We calculate the global structure of a dynamo-generated magnetic field of an accretion disk with surrounding halo of finite magnetic diffusivity. If the halo rotation law is fixed it remains to calculate a self-consistent model concerning the rotation law in the corona. For a Keplerian disk the effective potential at a point on a field line, corotating with the footpoint R_0, is

$$\psi = -\frac{GM_*}{R_0}\left[\frac{R_0}{(R^2+Z^2)^{1/2}} + \frac{1}{2}\left(\frac{R}{R_0}\right)^2\right]. \qquad (48)$$

Blandford & Payne (1982) showed that there is a characteristic angle of launching cold winds or jets. If the inclination angle between the vertical and the field line at the disk surface is greater than 30° the equilibrium at $R = R_0$ is unstable. If the angle is smaller than 30° there exists a potential barrier such that the equilibrium is stable.

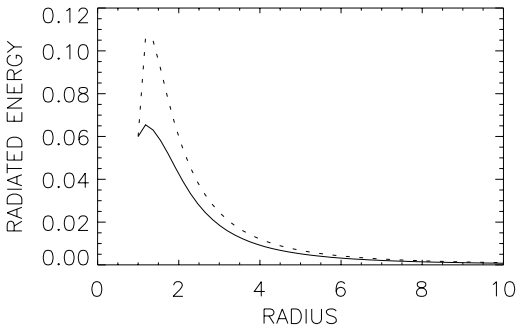

Fig. 8. Negative dynamo number ($c_\alpha = -1$): The surface energy flux $\sigma T_{\rm eff}^4$ in units of $\Omega_{\rm K*}^2 \dot{M}/2\pi$ for the magnetized disk (solid) and the non-magnetized disk (dotted)

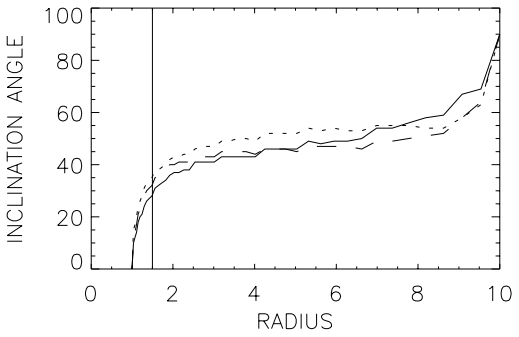

Fig. 9. The inclination of the poloidal field to the vertical at the disk surface for $\mathrm{Pm} = 1$. Note the saturation of the angle at about 45° in the inner part of the disk. $\epsilon = 100$ (solid), $\epsilon = 10$ (dashed), $\epsilon = 1$ (dotted)

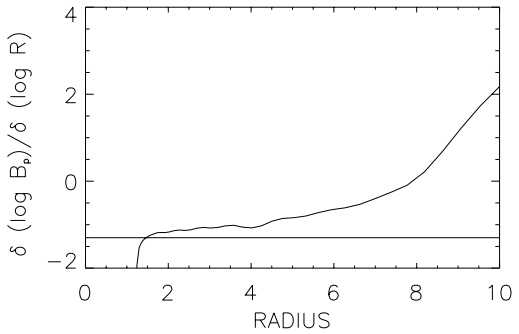

Fig. 10. The radial dependency of the poloidal magnetic field at the disk surface. It is $\bar{B}_{\rm p} \propto R^{-\mu}$ with $\mu \leq 1.3$. $\mathrm{Pm} = 1, \alpha_{\rm SS} = 0.01$

Ogilvie & Livio (1998) showed that a certain potential difference must be overcome even for an angle greater than 30° if the magnetic field is flattening the rotation law. The potential difference is minimized for an angle of 38°. They proposed that there has to be an additional source of energy to launch an outflow from a magnetized disk.

Our disk dynamo-model for $c_\alpha = -1$ shows no dependence of the inclination angle on the ratio $\epsilon = \eta_{\rm out}/\eta_{\rm disk}$ of the magnetic diffusivities between halo and disk (Fig. 9). There exists a broad region where the inclination angle is big enough ($\approx 45^\circ$) such that a magnetically driven wind or jet is possible (cf. Campbell et al. 1998). Only in the innermost region (less than 1.5 stellar radii) the matter has to overcome an additional potential difference. The reason is the radial distribution of the poloidal field in the disk, which is determined by the radial distribution of the equipartition value in our model. The magnetic field dragging by the accretion flow has a dominant influence on the inclination only for a magnetic Prandtl number $\gg 1$ (Reyes-Ruiz & Stepinski 1996, 1997). This dynamo seems to be compatible with the known jet solutions. However, it would be interesting to investigate the dynamo with a real centrifugally driven outflow with different quenching functions to see how far the disk field is really responsible for the jet launching.

5.2. Poloidal collimation

Spruit et al. (1997) argue that the toroidal fields are too unstable to contribute significantly to collimation. Moreover they have shown that the jet would be decollimated if the toroidal field is the only collimation mechanism. They propose that the collimation mechanism of a jet is due to the magnetic pressure of a poloidal field anchored in the disk where the radial profile is of great importance. They have derived the criterion that $\bar{B}_{\rm p} \propto R^{-\mu}$ with $\mu \leq 1.3$ is sufficient. In opposition to Torkelsson & Brandenburg (1994b) we show that it is indeed possible to generate steady large-scale fields of fixed (dipolar) polarity with a radial decay of the poloidal field like $\bar{B}_{\rm p} \propto R^{-\mu}, \mu \leq 1.3$ (Fig. 10).

Acknowledgements. We are grateful to acknowledge the support of the work of M. v. R. by the Deutsche Forschungsgemeinschaft (DFG) as well as numerous intensive discussions with C.G. Campbell during his summer visit in Potsdam. We wish to thank the referee, A. Brandenburg, for his detailed comments which helped to improve the paper.

References

Blandford R.D., Payne D.G., 1982, MNRAS 199, 883
Brandenburg A., Donner K.J., 1997, MNRAS 288, L29
Brandenburg A., Campbell C.G., 1998, MNRAS 298, 223
Campbell C.G., 1997, Magnetohydrodynamics in binary stars. Kluwer, Dordrecht
Campbell C.G., Papaloizou J.C.B., Agapitou V., 1998, MNRAS 300, 315
Campbell C.G., 1999, Geophys. Astrophys. Fluid Dyn. 90, 113
Dobler W., Poezd A., Shukurov A., 1996, A&A 312, 663
Duschl W.J., Tscharnuter W.M., 1991, A&A 241, 153
Horne K., 1993, Eclipse mapping of accretion disks. The first decade. In: Wheeler J.C. (ed.) Accretion disks in compact stellar systems. World Scientific Publishing, p. 117
Kitchatinov L.L., 1991, A&A 243, 483
Kitchatinov L.L., Pipin V.V., Rüdiger G., 1994, Astron. Nachr. 315, 157
Kley W., 1989, A&A 222, 141
Kley W., Lin D.N.C., 1992, ApJ 397, 600
Livio M., Pringle J.E., 1992, MNRAS 259, 23
Meyer F., Meyer-Hofmeister E., 1982, A&A 106, 34
Ogilvie G.I., Livio M., 1998, ApJ 499, 329
Pringle J.E., 1981, ARA&A 19, 137
Regev O., Bertout C., 1995, MNRAS 272, 71

Rekowski v. M., Fröhlich H.-E., 1997, A&A 319, 225
Reyes-Ruiz M., Stepinski T.F., 1996, ApJ 459, 653
Reyes-Ruiz M., Stepinski T.F., 1997, MNRAS 285, 501
Rüdiger G., Kitchatinov L.L., 1993, A&A 269, 581
Rüdiger G., Kitchatinov L.L., Küker M., Schultz M., 1994, Geophys. Astrophys. Fluid Dyn. 78, 247
Rüdiger G., Elstner D., Stepinski T.F., 1995, A&A 298, 934
Rüdiger G., Schultz M., 1997, A&A 319, 781
Shakura N.I., Sunyaev R.A., 1973, A&A 24, 337
Smak J., 1984, Acta Astron. 34, 161
Spruit H.C., Foglizzo T., Stehle R., 1997, MNRAS 288, 333
Stepinski T.F., Levy E.H., 1990, ApJ 362, 318
Torkelsson U., Brandenburg A., 1994a, A&A 283, 677
Torkelsson U., Brandenburg A., 1994b, A&A 292, 341
Wang Y.-M., 1995, ApJ 449, 153
Wang Y.-M., 1997, ApJ 487, L85